Letter

X-ray mirrors on flexible polymer substrates fabricated by atomic layer deposition

Abstract

Atomic layer deposition (ALD) techniques were used to fabricate W/Al_2O_3 superlattices with high X-ray reflectivity on flexible Kapton® polyimide and polyethylene naphthalate (PEN) polymer substrates. Reflectivities of 78% and 74% at $\lambda = 1.54$ Å were measured for 6-bilayer W/Al_2O_3 superlattices on Kapton® polyimide and PEN, respectively. These excellent X-ray reflectivities are attributed to precise bilayer thicknesses and ultrasmooth interfaces obtained by ALD and smoothing of the initial polymer surface by an Al_2O_3 ALD layer. The conformal ALD film growth also produces correlated roughness that enhances the reflectivity. These W/Al_2O_3 superlattices on flexible polymers should be useful for ultralight and adjustable radius of curvature X-ray mirrors.
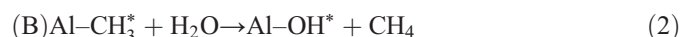© 2007 Published by Elsevier B.V.

Lightweight and flexible X-ray mirrors may be useful for a variety of applications. Flexible X-ray mirrors could replace toroidally bent crystals to provide adjustable curvatures for X-ray focusing [1,2]. The ease of manipulating a flexible mirror could also facilitate the design of adaptive X-ray mirrors [3]. Lightweight X-ray mirrors with low mass areal density are required for X-ray observatory missions [4,5]. In addition, flexible X-ray mirrors for X-ray spectrometry in space are required for mounting on substrates to obtain the proper telescope geometries [6].

The fabrication of lightweight and flexible X-ray mirrors is possible using atomic layer deposition (ALD) techniques to fabricate superlattice structures on polymer substrates. ALD uses sequential, self-limiting half-reactions between gas precursors and a solid surface to deposit conformal and ultrasmooth thin films with an atomic level thickness control [7,8]. Previous work has shown that precise thickness control and conformal deposition can yield W/Al_2O_3 superlattices with an extremely high reflectivity of 96.5% at $\lambda = 1.54$ Å [9]. This paper expands on the previous work and shows that W/Al_2O_3 superlattices with high reflectivity can also be grown on flexible polymeric substrates.

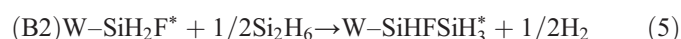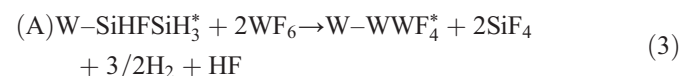W/Al_2O_3 nanolaminates have been previously grown by ALD at 177 °C and have displayed unique thermal [10] and optical [11] properties. The ALD of W/Al_2O_3 nanolaminates has also been demonstrated on polysilicon micromirrors [12] and carbon nanotubes [13]. In this work, the growth temperature was reduced to 125 °C to avoid damaging the polymer substrates. Al_2O_3 ALD growth was performed using trimethylaluminum, $Al(CH_3)_3$, and water according to the following two surface reactions [14,15]:

$$(A) \quad Al-OH^* + Al(CH_3)_3 \rightarrow Al-O-Al(CH_3)_2^* + CH_4 \qquad (1)$$

$$(B) \quad Al-CH_3^* + H_2O \rightarrow Al-OH^* + CH_4 \qquad (2)$$

where the asterisks denote the surface groups. At 125 °C, the growth rate for Al_2O_3 ALD is ~ 1.2 Å per AB cycle [16]. Including the purging periods following each reactant, each AB cycle required 44 s.

W ALD growth was also performed at 125 °C using tungsten hexafluoride, WF_6, and disilane, Si_2H_6. Silicon from Si_2H_6 serves as a sacrificial species on the surface to reduce the W without incorporating in the resulting film [17]. The surface reactions presented below have been determined from mass spectrometry [18] and quartz crystal microbalance experiments [19]:

$$(A) \quad W-SiHFSiH_3^* + 2WF_6 \rightarrow W-WWF_4^* + 2SiF_4 + 3/2H_2 + HF \qquad (3)$$

$$(B1) \quad W-F_4^* + Si_2H_6 \rightarrow W-SiH_2F^* + SiHF_3 + 3/2H_2 \qquad (4)$$

$$(B2) \quad W-SiH_2F^* + 1/2Si_2H_6 \rightarrow W-SiHFSiH_3^* + 1/2H_2 \qquad (5)$$

The growth rate for W ALD at 125 °C is ~ 4.0 Å/cycle after nucleation [9]. Each W ALD cycle required 61 s.

The ALD W/Al_2O_3 nanolaminate growth was performed in a viscous flow ALD reactor operating at a N_2 carrier gas pressure

Report Documentation Page

1. REPORT DATE **2007**	2. REPORT TYPE	3. DATES COVERED **00-00-2007 to 00-00-2007**

4. TITLE AND SUBTITLE	5a. CONTRACT NUMBER
X-ray mirrors on flexible polymer substrates fabricated by atomic layer deposition	5b. GRANT NUMBER
	5c. PROGRAM ELEMENT NUMBER
6. AUTHOR(S)	5d. PROJECT NUMBER
	5e. TASK NUMBER
	5f. WORK UNIT NUMBER

7. PERFORMING ORGANIZATION NAME(S) AND ADDRESS(ES) **University of Colorado,Department of Chemistry and Biochemistry,Boulder,CO,80309**	8. PERFORMING ORGANIZATION REPORT NUMBER

9. SPONSORING/MONITORING AGENCY NAME(S) AND ADDRESS(ES)	10. SPONSOR/MONITOR'S ACRONYM(S)
	11. SPONSOR/MONITOR'S REPORT NUMBER(S)

12. DISTRIBUTION/AVAILABILITY STATEMENT
Approved for public release; distribution unlimited

13. SUPPLEMENTARY NOTES

14. ABSTRACT
see report

15. SUBJECT TERMS

16. SECURITY CLASSIFICATION OF:			17. LIMITATION OF ABSTRACT	18. NUMBER OF PAGES	19a. NAME OF RESPONSIBLE PERSON
a. REPORT **unclassified**	b. ABSTRACT **unclassified**	c. THIS PAGE **unclassified**	**Same as Report (SAR)**	**4**	

Fig. 1. Schematic of 6-bilayer W/Al$_2$O$_3$ superlattice deposited at 125 °C on Kapton® polyimide, PEN and silicon substrates.

Fig. 3. TEM image of 6-bilayer W/Al$_2$O$_3$ superlattice on Kapton® polyimide. Higher magnification view reveals well-defined W/Al$_2$O$_3$ superlattice structure.

of ~133 Pa [20]. Three different substrates were introduced in the deposition chamber and coated at the same time. The polymer substrates were 5.08 cm × 2.54 cm Kapton® polyimide and polyethylene naphthalate (PEN) substrates obtained from DuPont. A 5.08 cm × 2.54 cm silicon wafer was used as a reference substrate. A buffer layer of 100 cycles of Al$_2$O$_3$ ALD was first grown directly on the substrates at 125 °C to smooth the underlying polymer surface and provide a seed layer for the W ALD layer. X-ray reflectivity (XRR) analysis indicated that this Al$_2$O$_3$ ALD buffer layer had a thickness of ~95 Å on Kapton® polyimide and PEN and ~110 Å on silicon. The smaller thicknesses on the polymer substrates result from the 10–15 AB cycles that are required for Al$_2$O$_3$ ALD nucleation on polymers [21].

A 6-bilayer W/Al$_2$O$_3$ nanolaminate was then grown on top of the ALD Al$_2$O$_3$ buffer layer as illustrated in Fig. 1. Each bilayer consisted of 15 AB cycles for W ALD and 49 AB cycles for Al$_2$O$_3$ ALD. Based upon nucleation results for

W ALD on Al$_2$O$_3$ ALD surfaces [9], 15 AB cycles for W ALD should yield a total thickness of 42 Å. Likewise, 49 AB cycles for Al$_2$O$_3$ ALD should yield a total thickness of ~59 Å [16]. A structural investigation of the W/Al$_2$O$_3$ nanolaminates provided evidence for thin interlayers at each interface containing silicon species. These interlayers add a total of ~10 Å per bilayer. Consequently, the spacer layer thickness was ~70 Å and the W ALD thickness was ~43 Å as determined by XRR analysis. The total thickness of the 6-bilayer multilayer was ~675 Å.

Fig. 2 shows a picture of a PEN substrate before and after deposition of the 6-bilayer W/Al$_2$O$_3$ superlattice. The original PEN substrate on the left is transparent. The coated

Fig. 2. Picture of flexible PEN substrate before and after deposition of 6-bilayer W/Al$_2$O$_3$ superlattice.

Fig. 4. X-ray reflectivity scans at $\lambda = 1.54$ Å of 6-bilayer W/Al$_2$O$_3$ superlattices on silicon, Kapton® polyimide and PEN substrates.

PEN sample on the right illustrates that the 6-bilayer W/Al_2O_3 superlattice exhibits a high optical reflectivity in the visible resulting from the W films. In addition, Fig. 2 highlights the flexibility of the coated PEN sample without any peeling or cracking.

Transmission electron microscopy (TEM) observations have been performed on the 6-bilayer W/Al_2O_3 multilayers on Kapton® polyimide. These TEM images are shown in Fig. 3. The upper picture at low magnification confirms the presence of a well-defined W/Al_2O_3 superstructure. The dark layers are the W ALD layers and the light areas are the spacer layers. The bilayers are extremely conformal to the initial Kapton® polyimide surface. A higher magnification of the W/Al_2O_3 nanolaminate is shown in the lower image in Fig. 3. This picture confirms that the W ALD layers have a thickness of ~ 45 Å and the spacer layers have a thickness of ~ 70 Å.

Fig. 4 displays X-ray reflectivity (XRR) scans performed on the three different substrates. These scans were obtained using a Bede D1 high resolution X-ray diffractometer equipped with a copper X-ray tube operating at $\lambda = 1.54$ Å [9]. The X-ray tube current was 40 mA with a voltage of 40 kV. The slit defining the incident X-ray beam had a width of 0.25 mm. With this X-ray beam width, the X-ray beam slightly overfills the substrate length of 5.08 cm for reflection at the critical angle. This X-ray beam width was necessary for sufficient sensitivity.

The REFS genetic algorithm fitting software from Bede X-ray Metrology was employed to obtain film thicknesses and X-ray reflectivities. The fitting accounts for slightly overfilling the substrate at the critical angle. The XRR scan for the W/Al_2O_3 nanolaminate grown on the reference silicon substrate exhibits the expected Bragg peaks that reveal the presence of a superstructure. $N-2$ Kiessig fringes are in between each Bragg peak where N is the number of bilayers in the superstructure. A measured reflectivity of 80% is obtained for the first Bragg peak from this 6-bilayer W/Al_2O_3 superlattice on the silicon wafer. Higher reflectivities result from W/Al_2O_3 superlattices with 16-bilayers [9].

The Bragg peaks are still present for the 6-bilayer W/Al_2O_3 superlattices deposited on the Kapton® polyimide and PEN substrates. These Bragg peaks confirm the superlattice structure observed by TEM. The measured reflectivities for the first Bragg peaks were 78% and 74% on Kapton® polyimide and PEN, respectively. These high reflectivities are independent of flexing and are very close to the reflectivity of 80% on the silicon wafer. In addition, the superlattice peaks occur at the same angular positions as observed on the silicon wafer. This behavior is consistent with the same bilayer thickness on the silicon and polymer substrates. The Kiessig fringes are less intense on Kapton® polyimide and almost absent on PEN. This trend can be attributed to the slight curvature of the Kapton® polyimide and PEN substrates. The polymer substrates may not be perfectly planar on the substrate holder because of their flexibility.

The excellent X-ray reflectivity on the polymeric substrates is attributed to the precise bilayer thicknesses obtained by ALD processing. The high X-ray reflectivity also results from the smoothing of the initial polymer surface by the Al_2O_3 ALD buffer layer with a thickness of ~ 100 Å. This Al_2O_3 ALD layer is known to deposit extremely conformally on trenched structures [22]. This conformal deposition can fill in surface roughness on the polymer surface that occurs with a lateral dimension of ≤ 200 Å.

The ALD growth will also produce ultrasmooth interfaces because the self-limiting surface chemistry during ALD allows every surface reaction to reach completion. This growth mechanism prevents randomness in the deposition process that can lead to interfacial roughness [9]. The conformality of ALD also ensures that any roughness is correlated and will propagate through the entire W/Al_2O_3 multilayer. This correlated roughness should not significantly decrease the specular reflectivity at the Bragg condition [23].

ALD has the potential to fabricate very lightweight, flexible and high reflectivity X-ray mirrors on polymeric substrates. These X-ray mirrors could be very useful for X-ray focusing, adaptive X-ray mirrors and future X-ray observatory missions in space. Because ALD is based on gas precursors, ALD processing methods are scalable to larger substrates and can be used to coat many substrates in parallel. In addition, the W/Al_2O_3 superlattices on polymer substrates could become "free standing" with the removal of the underlying polymer. This "free standing" W/Al_2O_3 superlattice would provide an X-ray mirror with the lowest mass areal density.

References

[1] T. Missalla, I. Uschmann, E. Forster, G. Jenke, D. Von der Linde, Rev. Sci. Instrum. 70 (1999) 1288.
[2] S.G. Podorov, A. Nazarkin, E. Forster, Opt. Commun. 259 (2006) 696.
[3] J. Susini, R. Baker, M. Krumrey, W. Schwegle, A. Kvick, Rev. Sci. Instrum. 66 (1995) 2048.
[4] N.E. White, H. Tananbaum, Proc. SPIE 4851 (2003) 293.
[5] W.W. Zhang, D.A. Content, S.J. Henderson, J.P. Lehan, R. Petre, T.T. Saha, S.L. O'Dell, W.D. Jones, W.A. Podgorski, P.B. Reid, Proc. SPIE 5488 (2004) 820.
[6] W. Zhang, D. Content, T. Saha, R. Petre, S. O'Dell, W. Jones, W. Davis, W. Podgorski, Proc. SPIE 5168 (2004) 168.
[7] S.M. George, A.W. Ott, J.W. Klaus, J. Phys. Chem. 100 (1996) 13121.
[8] M. Ritala, M. Leskela, in: H.S. Nalwa (Ed.), Atomic Layer Deposition, Handbook of Thin Film Materials, Academic Press, San Diego, CA, 2001.
[9] F.H. Fabreguette, R.A. Wind, S.M. George, Appl. Phys. Lett. 88 (2006) 013116.
[10] R.M. Costescu, D.G. Cahill, F.H. Fabreguette, Z.A. Sechrist, S.M. George, Science 303 (2004) 989.
[11] Z.A. Sechrist, F.H. Fabreguette, O. Heintz, T.M. Phung, D.C. Johnson, S.M. George, Chem. Mater. 17 (2005) 3475.
[12] M.K. Tripp, F.H. Fabreguette, C.F. Herrmann, S.M. George, V.M. Bright, Proc. SPIE 5720 (2005) 241.
[13] C.F. Herrmann, F.H. Fabreguette, D.S. Finch, R. Geiss, S.M. George, Appl. Phys. Lett. 87 (2005) 123110.

[14] A.W. Ott, J.W. Klaus, J.M. Johnson, S.M. George, Thin Solid Films 292 (1997) 135.
[15] A.C. Dillon, A.W. Ott, J.D. Way, S.M. George, Surf. Sci. 322 (1995) 230.
[16] M.D. Groner, F.H. Fabreguette, J.W. Elam, S.M. George, Chem. Mater. 16 (2004) 639.
[17] J.W. Klaus, S.J. Ferro, S.M. George, Thin Solid Films 360 (2000) 145.
[18] R.K. Grubbs, N.J. Steinmetz, S.M. George, J. Vac. Sci. Technol., B 22 (2004) 1811.
[19] F.H. Fabreguette, Z.A. Sechrist, J.W. Elam, S.M. George, Thin Solid Films 488 (2005) 103.
[20] J.W. Elam, M.D. Groner, S.M. George, Rev. Sci. Instrum. 73 (2002) 2981.
[21] C.A. Wilson, R.K. Grubbs, S.M. George, Chem. Mater. 17 (2005) 5625.
[22] M. Ritala, M. Leskela, J.P. Dekker, C. Mutsaers, P.J. Soininen, J. Skarp, Chem. Vap. Depos. 5 (1999) 7.
[23] D.E. Savage, J. Kleiner, N. Schimke, Y.H. Phang, T. Jankowski, J. Jacobs, R. Kariotis, M.G. Lagally, J. Appl. Phys. 69 (1991) 1411.

Francois H. Fabreguette[a]
Steven M. George[a,b,*]

[a] *Department of Chemistry and Biochemistry, University of Colorado, Boulder, CO 80309-0215, USA*
[b] *Department of Chemical and Biological Engineering, University of Colorado, Boulder, CO 80309-0424, USA*

*Corresponding author. Department of Chemistry and Biochemistry, University of Colorado, Boulder, CO 80309-0215, USA. Tel.: +1 303 492 3398; fax: +1 303 492 5894.
E-mail address: Steven.George@Colorado.Edu.

18 September 2006